Vol. 19, No. 2 (2020) 697-712
Revista Mexicana de Ingeniería Química

# Sequential synthesis of PID controllers based on LQR method

# Síntesis secuencial de controladores PID basada en el método LQR

M.A. Hernández-Osorio[1], C.E. Ochoa-Velasco[2], M.A. García-Alvarado[3], A. Escobedo-Morales[1], and I.I. Ruiz-López[1*]

[1] *Facultad de Ingeniería Química. Benemérita Universidad Autónoma de Puebla. Av. San Claudio y 18 Sur. Ciudad Universitaria. C.P. 72570. Puebla, Puebla. México.*
[2] *Facultad de Ciencias Químicas. Benemérita Universidad Autónoma de Puebla. Av. San Claudio y 18 Sur. Ciudad Universitaria. C.P. 72570. Puebla, Puebla. México.*
[3] *Unidad de Investigación y Desarrollo en Alimentos. Instituto Tecnológico de Veracruz. Av. M.A. de Quevedo 2779. C.P. 91860. Veracruz, Veracruz. México.*

Received: October 22, 2019; Accepted:

## Abstract

The linear quadratic regulator (LQR) method is generalized to allow synthesis of PID controllers in MIMO processes. The proposed method is sequentially applied to produce proportional, integral and derivative actions. Three major usages are conceived for the proposed methodology: (i) ≪de novo≫ design of PID controllers, (ii) addition of derivative action to existing PI controllers and (iii) diagonalization of PID gain matrices. The two last procedures can be applied to controllers designed with different methodologies. The developed method was applied to the ≪de novo≫ design of a centralized PID controller for a three input-three output distillation column as well as the addition of derivative action to existing both centralized and multiloop PI controllers for a nonlinear continuous stirred tank reactor (CSTR). The proposed LQR method allowed the synthesis of centralized and multiloop PID controllers with better characteristics for set-point tracking, disturbance rejection, limited use of control signal and insensitivity to plant model uncertainty than those reported by other authors.

*Keywords*: Lyapunov function, quadratic index, quadratic optimal control, robust control, state-space model.

## Resumen

Se generalizó el método de reguladores lineales cuadráticos (LQR, por sus siglas en inglés) para permitir la síntesis de controladores PID en procesos con múltiples entradas y múltiples salidas. El método propuesto se aplica secuencialmente para producir las acciones proporcional, integral y derivativa. Se conciben tres usos principales para la metodología propuesta: (i) el diseño ≪de novo≫ de controladores PID, (ii) la adición de la acción derivativa a controladores PI existentes y (iii) la diagonalización de las matrices de ganancias PID. Adicionalmente, los dos últimos procedimientos se pueden aplicar a controladores diseñados con diferentes metodologías. El método desarrollado se aplicó al diseño ≪de novo≫ de un controlador centralizado PID para columna de destilación de tres entradas-tres salidas así como a la adición de la acción derivativa a controladores existentes PI centralizados y multilazo para un reactor continuo de tanque agitado (CSTR, por sus siglas en inglés) no lineal. El método LQR propuesto permitió la síntesis de controladores PID centralizados y multilazo con mejores características de seguimiento de referencia, rechazo a perturbaciones, uso limitado de la señal de control e insensibilidad a incertudumbre en el modelo de la planta que aquellos reportados por otros autores.

*Palabras clave*: control óptimo cuadrático, control robusto, modelo en espacio de estados, función de Lyapunov, índice cuadrático.

## 1 Introduction

Nowadays, proportional-integral (PI) and proportional-integral-derivative (PID) algorithms are the preferred control methods for most modern industrial processes because they have a simple structure and can be designed to exhibit both good performance and robustness characteristics (Flores-Estrella *et al*., 2016; Salazar-Pereyra *et al*., 2016; Estévez-Sánchez *et al*., 2017; Besta *et al*., 2018; Cruz-Rojas *et al*., 2019; Ma *et al*., 2019).

* *Corresponding author. E-mail*: irving.ruiz@correo.buap.mx
*Tel. +52-22-22-29-55-00x7250, Fax +52-22-22-29-55-00x7251*
https://doi.org/10.24275/rmiq/Sim814
*issn-e*: 2395-8472

However, when processes have multiple-input/multiple-output (MIMO) dynamics with complex interactions among variables, such as most chemical processes (Pathiran and Jagadeesan, 2018), the design of PI/PID controllers simultaneously achieving a correct control system operation (adequate set-point tracking, disturbance rejection and insensibility to model uncertainty) is not an easy task (Liu *et al*., 2010; Maghade and Patre, 2012; Ram and Chidambaram, 2015; Besta *et al*., 2018); moreover, the application of tuning methods developed for single-input/single-output (SISO) plants to individual control loops may compromise performance and stability (Vu and Lee, 2010; Nandong and Zang, 2014).

The quadratic optimal control is a state-space design methodology based on determining a multivariate feedback controller (a.k.a. linear quadratic regulator or LQR), through minimization of a quadratic performance index of both control and state variables (Estévez-Sánchez *et al*., 2017). The trade-off between the acceptable deviation in the trajectories of the state variables and control signals is adjusted by the elements of two weighting matrices (Das *et al*., 2013). The LQR approach can be also used to obtain output feedback (proportional) or PI controllers. For MIMO processes, the controllers produced by using the LQR approach have a centralized structure, and recent studies have demonstrated that LQR method can be applied to obtain diagonal PI control structures (Estévez-Sánchez *et al*., 2017). However, the synthesis of controllers including the derivative action via the LQR method is restricted to SISO plants based on first and second order plus time delays transfer functions (He *et al*., 2000; Srivastava *et al*., 2016).

The number of adjustable parameters for an $o \times o$ square MIMO process using a centralized PID controller is $3 \times o \times o$. Thus, the PID control design for a $2 \times 2$ MIMO system involves the tuning of 12 parameters, but the number of involved variables increases up to 27 and 48 for $3 \times 3$ and $4 \times 4$ MIMO processes, respectively. It is clear that the optimization problem of finding the control parameters set achieving process stability as well as some other performance measures quickly escalates in size and complexity (Pathiran and Jagadeesan, 2018), specially when considering that no previous information about the feasible solution space is known. This problem can be simplified by considering a multiloop control whenever the process allows for it or existing control hardware does not have the capacity to implement the centralized structure. In this case, an $o \times o$ MIMO process only has $3 \times o$ adjustable gains. However, as opposed to other methods such as the covariance matrix adaptation evolution strategy (Iruthayarajan and Saskar, 2010) or the preference ranking organization methods for enrichement evaluations (Rodríguez-Mariano *et al*., 2015), the searching task for optimal parameters in LQR methodology does not directly occur in the original space of controller gains but in the space of weighting matrix elements and full centralized $o \times o$ PI controllers can be obtained by adjusting as few as $o$ parameters in single or sequential steps (Estévez-Sánchez *et al*., 2017), vastly reducing the dimension of the optimization problem.

The objective of this work is to generalize the LQR methodology to allow the synthesis of full centralized PID controllers with good performance and robustness characteristics. This method is based on the sequential synthesis of proportional, integral and derivative actions with $o$ adjustable parameters in each step. Furthermore, the addition of derivative action to existing PI controllers as well as the diagonalization of PID gain matrices are also considered.

## 2 Theory

### 2.1 *Outline of the studied system*

The following linear time-invariant (LTI) system is able to represent a wide range of chemical engineering processes equipped with a linear controller:

$$\dot{\mathbf{x}} = \mathbf{a}\mathbf{x} + \mathbf{b}_1\mathbf{w} + \mathbf{b}_2\mathbf{u} \tag{1}$$

$$\mathbf{y} = \mathbf{c}\mathbf{x} + \mathbf{d}_1\mathbf{w} + \mathbf{d}_2\mathbf{u} \tag{2}$$

$$\dot{\boldsymbol{\xi}} = \boldsymbol{\alpha}\boldsymbol{\xi} + \boldsymbol{\beta}\mathbf{e} \tag{3}$$

$$\mathbf{u} = \boldsymbol{\gamma}\boldsymbol{\xi} + \boldsymbol{\delta}\mathbf{e} + \mathbf{K}_I\mathbf{q} \tag{4}$$

$$\mathbf{q} = \int_0^t \mathbf{e}dt \tag{5}$$

$$\mathbf{e} = \mathbf{r} - \mathbf{y} \tag{6}$$

where $\mathbf{x} \in \mathbb{R}^{n\times 1}$, $\mathbf{w} \in \mathbb{R}^{s\times 1}$, $\mathbf{u} \in \mathbb{R}^{c\times 1}$, $\mathbf{y} \in \mathbb{R}^{o\times 1}$, $\mathbf{q} \in \mathbb{R}^{o\times 1}$, $\mathbf{r} \in \mathbb{R}^{o\times 1}$ and $\boldsymbol{\xi} \in \mathbb{R}^{s\times 1}$ are the system state,

exogenous signal, control, measured output, output error, set-point and control state vectors, respectively. Here, $\mathbf{a} \in \mathbb{R}^{n\times n}$, $\mathbf{b}_1 \in \mathbb{R}^{n\times m}$, $\mathbf{b}_2 \in \mathbb{R}^{n\times c}$, $\mathbf{c} \in \mathbb{R}^{o\times n}$, $\mathbf{d}_1 \in \mathbb{R}^{o\times m}$, $\mathbf{d}_2 \in \mathbb{R}^{o\times c}$, $\boldsymbol{\alpha} \in \mathbb{R}^{s\times s}$, $\boldsymbol{\beta} \in \mathbb{R}^{s\times o}$, $\boldsymbol{\gamma} \in \mathbb{R}^{c\times s}$, $\boldsymbol{\delta} \in \mathbb{R}^{c\times o}$ and $\mathbf{K}_I \in \mathbb{R}^{o\times c}$. Eqs. (3)-(4) are able to represent a wide range of linear controllers with proportional, integral and derivative actions, as follows:

- Proportional (P) control.

$$\boldsymbol{\alpha} = \mathbf{0}; \quad \boldsymbol{\beta} = \mathbf{0}; \quad \boldsymbol{\gamma} = \mathbf{0}; \quad \boldsymbol{\delta} = \mathbf{K}_P; \quad \mathbf{K}_I = \mathbf{0} \tag{7}$$

- Proportional-integral (PI) control.

$$\boldsymbol{\alpha} = \mathbf{0}; \quad \boldsymbol{\beta} = \mathbf{0}; \quad \boldsymbol{\gamma} = \mathbf{0}; \quad \boldsymbol{\delta} = \mathbf{K}_P \tag{8}$$

- Proportional-integral-derivative (PID) control with filter. Eqs. (3) and (4) do not allow representation of improper transfer functions such as the ideal PID controller. Thus, PID structure must be modified with a filter to turn it into a proper function. However, since controller gains are not contained in a single matrix such as $\mathbf{K}_P$ or $\mathbf{K}_I$, the state-space representation of this structure is not as straightforward as for the P or PI controls. The transfer function of a PID controller with filter relating the $i$-th control variable with the $j$-th error signal is given by

$$\frac{u_i(s)}{e_j(s)} = \left(k_{Pij} + \frac{k_{Iij}}{s} + k_{Dij}s\right)\left(\frac{1}{\tau_{ij}s+1}\right) \tag{9}$$

The above equation has the following state-space observable canonical form representation

$$\frac{d\xi_{ij}}{dt} = \alpha_{ij}\xi_{ij} + \beta_{ij}e_j \tag{10}$$

$$u_i = \gamma_{ij}\xi_{ij} + \delta_{ij}e_j + k_{Iij}q_j \tag{11}$$

$$\alpha_{ij} = -1/\tau_{ij}; \quad \beta_{ij} = 1; \quad \gamma_{ij} = \tfrac{k_{Pij}}{\tau_{ij}} - k_{Iij} - \tfrac{k_{Dij}}{\tau_{ij}^2};$$

$$\delta_{ij} = \tfrac{k_{Dij}}{\tau_{ij}} \tag{12}$$

The $i \times j$ controllers can be grouped in the state-space representation given by eqs. (3) and (4) with the following definitions

$$\boldsymbol{\alpha}_i^* = \text{diag}\left(\begin{bmatrix} \alpha_{i1} & \alpha_{i2} & \dots & \alpha_{io} \end{bmatrix}\right) \in \mathbb{R}^{o\times o} \tag{13}$$

$$\boldsymbol{\alpha} = \text{diag}\left(\begin{bmatrix} \boldsymbol{\alpha}_1^* & \boldsymbol{\alpha}_2^* & \dots & \boldsymbol{\alpha}_c^* \end{bmatrix}\right) \in \mathbb{R}^{co\times co} \tag{14}$$

$$\boldsymbol{\beta}_i^* = \text{diag}\left(\begin{bmatrix} \beta_{i1} & \beta_{i2} & \dots & \beta_{io} \end{bmatrix}\right) \in \mathbb{R}^{o\times o} \tag{15}$$

$$\boldsymbol{\beta}^T = \begin{bmatrix} \boldsymbol{\beta}_1^* & \boldsymbol{\beta}_2^* & \dots & \boldsymbol{\beta}_o^* \end{bmatrix} \in \mathbb{R}^{o\times co} \tag{16}$$

$$\boldsymbol{\gamma}_i^* = \begin{bmatrix} \gamma_{i1} & \gamma_{i2} & \dots & \gamma_{io} \end{bmatrix} \in \mathbb{R}^{1\times o} \tag{17}$$

$$\boldsymbol{\gamma} = \text{diag}\left(\begin{bmatrix} \boldsymbol{\gamma}_1^* & \boldsymbol{\gamma}_2^* & \dots & \boldsymbol{\gamma}_c^* \end{bmatrix}\right) \in \mathbb{R}^{c\times co} \tag{18}$$

$$\boldsymbol{\delta} = \begin{bmatrix} \delta_{11} & \dots & \delta_{1o} \\ \vdots & & \vdots \\ \delta_{c1} & \dots & \delta_{co} \end{bmatrix} \in \mathbb{R}^{c\times o} \tag{19}$$

$$\mathbf{K}_I = \begin{bmatrix} k_{I11} & \dots & k_{I1o} \\ \vdots & & \vdots \\ k_{Ic1} & \dots & k_{Ico} \end{bmatrix} \in \mathbb{R}^{c\times o} \tag{20}$$

## 2.2 *Outline of the LQR methodology*

Let us consider the following LTI system equipped with a full-state feedback controller

$$\dot{\mathbf{X}} = \mathbf{A}\mathbf{X} + \mathbf{B}_1\mathbf{W} + \mathbf{B}_2\mathbf{U} \tag{21}$$

$$\mathbf{Y} = \mathbf{C}\mathbf{X} \tag{22}$$

$$\mathbf{U} = -\mathbf{K}\mathbf{X} \tag{23}$$

where $\mathbf{X} \in \mathbb{R}^{N\times 1}$, $\mathbf{W} \in \mathbb{R}^{S\times 1}$, $\mathbf{U} \in \mathbb{R}^{C\times 1}$ and $\mathbf{Y} \in \mathbb{R}^{O\times 1}$ are the system state, exogenous signal, control and measured output. The system coefficients have dimensions $\mathbf{A} \in \mathbb{R}^{N\times N}$, $\mathbf{B}_1 \in \mathbb{R}^{N\times E}$, $\mathbf{B}_2 \in \mathbb{R}^{N\times C}$, $\mathbf{C} \in \mathbb{R}^{O\times N}$ and $\mathbf{K} \in \mathbb{R}^{C\times O}$. LQR methodology can be applied to obtain the optimal full-state feedback controller described in Eq. (23) by minimizing the infinite-horizon cost function

$$J = \int_0^\infty (\mathbf{X}^T\hat{\mathbf{Q}}\mathbf{X} + \mathbf{U}^T\hat{\mathbf{R}}\mathbf{U})dt \tag{24}$$

where $\hat{\mathbf{Q}} \in \mathbb{R}^{N\times N}$ is a positive-definite (or positive-semidefinite) matrix and $\hat{\mathbf{R}} \in \mathbb{R}^{C\times C}$ is a positive-definite matrix. The matrices $\hat{\mathbf{Q}}$ and $\hat{\mathbf{R}}$ modify the trade-off between permisible error and magnitude of

control signals, respectively. The optimal feedback gains are calculated as

$$\mathbf{K} = \hat{\mathbf{R}}^{-1}\mathbf{B}_2^T\mathbf{P} \tag{25}$$

where $\mathbf{P}$ is obtained from the solution of the algebraic Ricatti equation:

$$\mathbf{A}^T\mathbf{P} + \mathbf{P}\mathbf{A} + \mathbf{P}\mathbf{B}_2\hat{\mathbf{R}}\mathbf{B}_2\mathbf{P} + \hat{\mathbf{Q}} = \mathbf{0} \tag{26}$$

LQR methodology allows the estimation of classical P and PI controllers for system (1)-(6) by introducing proper variable definitions for $\mathbf{X}$, $\mathbf{W}$, $\mathbf{U}$, $\mathbf{Y}$, $\mathbf{A}$, $\mathbf{B}_1$, $\mathbf{B}_2$, $\mathbf{C}$, $\hat{\mathbf{Q}}$, $\hat{\mathbf{R}}$ and $\mathbf{K}$ as follows:

- Proportional (P) control.

$$\mathbf{X} = \mathbf{x}; \quad \mathbf{Y} = \mathbf{y}; \quad \mathbf{A} = \mathbf{a}; \quad \mathbf{B}_1 = \mathbf{b}_1; \quad \mathbf{B}_2 = \mathbf{b}_2;$$

$$\mathbf{C} = \mathbf{c}; \quad \mathbf{K} = \mathbf{K}_P\mathbf{c} \tag{27}$$

- Proportional (PI) control.

$$\mathbf{Y}^T = \begin{bmatrix} \mathbf{y} & \mathbf{q} \end{bmatrix}; \quad \mathbf{A} = \begin{bmatrix} \mathbf{a} & \mathbf{0} \\ -\mathbf{c} & \mathbf{0} \end{bmatrix};$$

$$\mathbf{C} = \begin{bmatrix} \mathbf{c} & \mathbf{0} \\ \mathbf{0} & \mathbf{I}_r \end{bmatrix}; \quad \mathbf{K} = \begin{bmatrix} -\mathbf{K}_P\mathbf{c} & \mathbf{K}_I \end{bmatrix} \tag{28}$$

- Integral action added to a P control (Estévez-Sanchez *et al*., 2017).

$$\mathbf{Y}^T = \mathbf{q}; \quad \mathbf{A} = \begin{bmatrix} \mathbf{a} - \mathbf{b}_2\mathbf{K}_P\mathbf{c} & \mathbf{0} \\ -\mathbf{c} & \mathbf{0} \end{bmatrix};$$

$$\mathbf{C} = \begin{bmatrix} \mathbf{0} & \mathbf{I}_r \end{bmatrix}; \quad \mathbf{K} = -\mathbf{K}_I\mathbf{C} \tag{29}$$

In the case of the one-step or sequential synthesis of integral action,

$$\mathbf{X}^T = \begin{bmatrix} \mathbf{x} & \mathbf{q} \end{bmatrix}; \quad \mathbf{B}_1 = \begin{bmatrix} \mathbf{b}_1 \\ \mathbf{0} \end{bmatrix}; \quad \mathbf{B}_2 = \begin{bmatrix} \mathbf{b}_2 \\ \mathbf{0} \end{bmatrix} \tag{30}$$

In all cases,

$$\mathbf{U} = \mathbf{u}; \quad \mathbf{W} = \mathbf{w}; \quad \hat{\mathbf{Q}} = \mathbf{C}^T\mathbf{Q}\mathbf{C}; \quad \hat{\mathbf{R}} = \mathbf{R} \tag{31}$$

### *2.3 Synthesis of derivative action via LQR approach*

Estévez-Sánchez *et al*. (2017) proposed that integral action could be sequentially applied to a plant already equipped with a P controller by using LQR methodology. For achieving this purpose, the plant is set in closed-loop with the proportional gains but it is left in open-loop with the integral action. In this work, the same idea is explored for the synthesis of derivative action; the plant is set in closed-loop with PI gains, while the derivative action is in open-loop. Thus, the following state-space representation is proposed:

$$\mathbf{Y} = \dot{\mathbf{y}}; \quad \mathbf{A} = \begin{bmatrix} \mathbf{a} - \mathbf{b}_2\mathbf{K}_P\mathbf{c} & \mathbf{b}_2\mathbf{K}_I \\ -\mathbf{c} & \mathbf{0} \end{bmatrix};$$

$$\mathbf{C} = [\mathbf{I}_r + \mathbf{c}\mathbf{b}_2\mathbf{K}_D]^{-1}\begin{bmatrix} -\mathbf{c}\mathbf{a} + \mathbf{c}\mathbf{b}_2\mathbf{K}_P\mathbf{c} & -\mathbf{c}\mathbf{b}_2\mathbf{K}_I \end{bmatrix};$$

$$\mathbf{K} = -\mathbf{K}_D\mathbf{C} \tag{32}$$

where the remaining variables are defined as in eqs. (30) and (31). Unlike the synthesis of the integral action, in this case the open-loop matrix $\mathbf{C}$ also contains the derivative gains. Thus, the following iterative procedure is proposed to the synthesis of the derivative action:

1. Assemble $\mathbf{A}$ and $\mathbf{B}_2$.
2. Initialize $\mathbf{K}_D = \mathbf{0}$.
3. Assemble $\mathbf{C}$ and $\hat{\mathbf{Q}}$.
4. Estimate $\mathbf{K}$ with Eq. (25) and then $\mathbf{K}_D$ from definition given in Eq. (32) as $\mathbf{K}_D = -\mathbf{K}\mathbf{C}^{-1}$.
5. Repeat steps (3)-(5) until $\mathbf{K}_D$ no longer changes between iterations.

Multiloop versions of centralized PID controllers can be obtained through a sequential method. The diagonalization of derivative gains matrix is based on its Jordan decomposition, extending the original method reported by Estévez-Sánchez *et al*. (2017) for PI gains. The method is as follows:

1. Assemble $\mathbf{A}$ and $\mathbf{B}_2$.
2. Initialize $\hat{\mathbf{R}} = \mathbf{I}$.
3. Assemble $\mathbf{C}$ and $\hat{\mathbf{Q}}$.
4. Solve Eq. (26) to get $\mathbf{P}$ and estimate $\mathbf{K}$ with Eq. (25).

5. Calculate $\mathbf{K}_D$ from definition given in Eq. (32) as $\mathbf{K}_D = -\mathbf{K}\mathbf{C}^{-1}$.
6. Get the Jordan matrix decomposition of $\mathbf{K}_D$ as $\mathbf{K}_D = \mathbf{V}\mathbf{D}\mathbf{V}^{-1}$ where $\mathbf{D}$ and $\mathbf{V}$ contain the eigenvalues and eigenvectors of $\mathbf{K}_D$.
7. Set $\mathbf{K}_D = \mathbf{D}$.
8. Calculate $\mathbf{K}_D$ from definition given in Eq. (32) as $\mathbf{K}_D = -\mathbf{K}\mathbf{C}^{-1}$.
9. Estimate $\hat{\mathbf{R}}$ from Eq. (25) as $\hat{\mathbf{R}} = \mathbf{B}_2^T\mathbf{P}\mathbf{K}^{-1}$
10. Repeat steps (4)-(9) until $\mathbf{K}_D$ no longer changes between iterations.

PI gain matrices can be diagonalized in the same way as reported by Estévez-Sánchez *et al*. (2017).

## 2.4 *Multivariable PID controller design for the Ogunnaike distillation column*

The proposed methodology was applied to the ≪de novo≫ design of a centralized PID controller for a three input-three output distillation column.

### 2.4.1 *Process model*

Consider a 19-plates distillation column to separate ethanol from water, having variable feed and side stream draw-off locations (Ogunnaike *et al*., 1983). This system has the following transfer matrix representation:

$$\mathbf{G}(s) = \begin{bmatrix} \frac{0.66e^{-2.6s}}{6.7s+1} & \frac{-0.61e^{-3.5s}}{8.64s+1} & \frac{-0.0049e^{-s}}{9.06s+1} \\ \frac{1.11e^{-6.5s}}{3.25s+1} & \frac{-2.36e^{-3s}}{5.0s+1} & \frac{-0.012e^{-1.2s}}{7.09s+1} \\ \frac{-34.68e^{-9.2s}}{8.15s+1} & \frac{46.2e^{-9.4s}}{10.9s+1} & \frac{0.87(11.61s+1)e^{-s}}{(3.89s+1)(18.8s+1)} \end{bmatrix} \tag{33}$$

The transfer matrix (33) was written in the state-space form of eqs. (1)-(2) where the delay terms were aproximated as a series of first order systems. The transportation lags of $u_1$, $u_2$ and $u_3$ were divided before approximation as $e^{-9.2s} = e^{-1.3s-1.3s-1.95s-1.95s-1.35s-1.35s}$, $e^{-9.4s} = e^{-1.5s-1.5s-0.5s-2s-1.95s-1.95s}$ and $e^{-1.2s} = e^{-0.5s-0.5s-0.2s}$, respectively. Thus, the largest delay chain for each control variable can be used to generate the shorter lag terms. For example, the partition of $e^{-9.2s}$ in $g_{31}(s)$ also produces the terms $e^{-2.6s}$ and $e^{-6.5s}$ required in $g_{11}(s)$ and $g_{21}(s)$, respectively. In this way, a total of 15 first order models were neccesary to approximate the 9 transportation lag terms in Eq. (33). The time constants of these auxiliary first order models represented between the 5.5 and 60% of the smallest one found in the original transfer functions of Eq. (33). In this case, $\mathbf{x} \in \mathbb{R}^{25\times1}$, $\mathbf{u} \in \mathbb{R}^{3\times1}$ and $\mathbf{y} \in \mathbb{R}^{3\times1}$. The non-zero elements of matrices $\mathbf{a} = \mathbf{f}^{-1}\hat{\mathbf{a}}$, $\mathbf{b}_2 = \mathbf{f}^{-1}\hat{\mathbf{b}}_2$ ($\mathbf{f}, \hat{\mathbf{a}} \in \mathbb{R}^{n\times n}$) and $\mathbf{C}$ are: $f_{1,1} = f_{2,2} = 1.3$, $f_{3,3} = 6.7$, $f_{4,4} = f_{5,5} = 1.95$, $f_{6,6} = 3.25$, $f_{7,7} = f_{8,8} = 1.35$, $f_{9,9} = 8.15$, $f_{10,10} = f_{11,11} = 1.5$, $f_{12,12} = 5$, $f_{13,13} = f_{19,19} = f_{20,20} = 0.5$, $f_{14,14} = 8.64$, $f_{15,15} = 2$, $f_{16,16} = f_{17,17} = 1.95$, $f_{18,18} = 10.9$, $f_{21,21} = 9.06$, $f_{22,22} = 3.89$, $f_{23,23} = 1$, $f_{24,24} = 0.2$, $f_{25,25} = 7.09$, $\hat{a}_{1,1} = \hat{a}_{2,2} = \hat{a}_{3,3} = \hat{a}_{4,4} = \hat{a}_{5,5} = \hat{a}_{6,6} = \hat{a}_{7,7} = \hat{a}_{8,8} = \hat{a}_{9,9} = \hat{a}_{10,10} = \hat{a}_{11,11} = a_{12,12} = a_{13,13} = a_{14,14} = a_{15,15} = \hat{a}_{16,16} = \hat{a}_{17,17} = \hat{a}_{18,18} = \hat{a}_{19,19} = \hat{a}_{20,20} = \hat{a}_{21,21} = \hat{a}_{22,22} = \hat{a}_{24,24} = \hat{a}_{25,25} = -1$, $\hat{a}_{2,1} = \hat{a}_{4,2} = \hat{a}_{5,4} = \hat{a}_{7,5} = a_{8,7} = a_{11,10} = a_{13,11} = a_{15,13} = \hat{a}_{16,15} = \hat{a}_{17,16} = \hat{a}_{20,19} = \hat{a}_{23,22} = a_{24,20} = 1$, $\hat{a}_{3,2} = 0.66$, $\hat{a}_{6,5} = 1.11$, $\hat{a}_{9,8} = -34.68$, $\hat{a}_{12,11} = -2.36$, $\hat{a}_{14,13} = -0.61$, $\hat{a}_{18,17} = 46.2$, $\hat{a}_{21,20} = -0.0049$, $\hat{a}_{22,20} = 0.87$, $\hat{a}_{23,23} = -1/18.8$, $\hat{a}_{25,24} = -0.012$, $b_{2,1,1} = b_{2,10,2} = b_{2,19,3} = 1$, $c_{1,3} = c_{1,14} = c_{1,21} = c_{2,6} = c_{2,12} = c_{2,25} = c_{3,9} = c_{3,18} = 1$, $c_{3,22} = 11.61/18.8$, $c_{3,23} = -1/18.8 - (1/18.8)(11.61/18.8)$. Matrices $\mathbf{b}_1$, $\mathbf{d}_1$ and $\mathbf{d}_2$ do not exist in this system.

### 2.4.2 *Screening of control weights for the synthesis of PID controllers*

Matrices $\mathbf{Q}$ and $\mathbf{R}$ were considered to be diagonal during the controller synthesis, a common choice in other studies dealing with LQR methodology (Das *et al*., 2013; Estévez-Sánchez *et al*., 2017). In this system, output $y_3$ (a temperature value) is not in the same magnitude order as outputs $y_1$ and $y_2$ (composition data). If $\mathbf{Q}$ is diagonal then

$$\int_0^\infty \mathbf{Y}^T\mathbf{Q}\mathbf{Y}dt = \sum_{i=1}^{O} q_{ii}\int_0^\infty Y_i^2 dt \tag{34}$$

Elements in $\mathbf{Q}$ must be chosen in such a way that each integral of squared output errors has the same magnitude order; thus, the ratio $q_{ii}/q_{33}$ ($i = 1, 2$) should be in the range of 10 to 100. In this study, controllers were obtained by exploring the resulting combinations of the diagonal elements in $\mathbf{R}$ in the following ranges:

- Synthesis of the proportional action

$$\mathbf{Q} = \begin{bmatrix} 100 & 0 & 0 \\ 0 & 100 & 0 \\ 0 & 0 & 1 \end{bmatrix};$$

$$\log_{10}\mathbf{R} = \begin{bmatrix} 0,\ldots,2 & 0 & 0 \\ 0 & 1,\ldots,3 & 0 \\ 0 & 0 & -2,\ldots,-1 \end{bmatrix} \tag{35}$$

- Synthesis of the integral action

$$\mathbf{Q} = \begin{bmatrix} 100 & 0 & 0 \\ 0 & 100 & 0 \\ 0 & 0 & 10 \end{bmatrix};$$

$$\log_{10}\mathbf{R} = \begin{bmatrix} 4,\ldots,6 & 0 & 0 \\ 0 & 5,\ldots,6 & 0 \\ 0 & 0 & -1,\ldots,3 \end{bmatrix} \tag{36}$$

- Synthesis of the derivative action

$$\mathbf{Q} = \begin{bmatrix} 100 & 0 & 0 \\ 0 & 100 & 0 \\ 0 & 0 & 1 \end{bmatrix};$$

$$\log_{10}\mathbf{R} = \begin{bmatrix} 1,\ldots,2 & 0 & 0 \\ 0 & 0,\ldots,1 & 0 \\ 0 & 0 & -2,\ldots,-1 \end{bmatrix} \tag{37}$$

A logarithmic step size of 0.1 (base 10) was considered in all cases.

### *2.4.3 2.4.3 Closed-loop indices for the selection of PID control*

Once the relative importance of each output is determined with **Q**, all LQR controllers minimize Eq. (24) for the selected control weight **R**. However, it is worth noting that the index (24) does not contain the *real* output or control signals, but it contains *extended* output or control signals *conveniently defined* to achieve the synthesis of the required control action (proportional, integral or derivative). Thus, the selection of the LQR controllers for different control weights must be further refined through estimating additional performance and robustness indices. These indices can be evaluated by considering the following closed-loop representation of the plant given by eqs. (1)-(6):

$$\mathbf{z} = \mathbb{A}\mathbf{z} + \mathbb{B}_1\mathbf{w} + \mathbb{B}_2\mathbf{r} \tag{38}$$

$$\mathbf{y} = \mathbb{C}_1\mathbf{z} + \mathbb{D}_{11}\mathbf{w} + \mathbb{D}_{12}\mathbf{r} \tag{39}$$

$$\mathbf{u} = \mathbb{C}_2\mathbf{z} + \mathbb{D}_{21}\mathbf{w} + \mathbb{D}_{22}\mathbf{r} \tag{40}$$

$$\mathbb{A} = \begin{bmatrix} \mathbf{a} - \mathbf{b_2}\boldsymbol{\delta}\Delta\mathbf{c} & \mathbf{b_2}\nabla\boldsymbol{\gamma} & \mathbf{b_2}\nabla\mathbf{K_I} \\ -\boldsymbol{\beta}\Delta\mathbf{c} & \boldsymbol{\alpha} - \boldsymbol{\beta}\Delta\mathbf{d}_2\boldsymbol{\gamma} & -\boldsymbol{\beta}\Delta\mathbf{d}_2\mathbf{K_I} \\ -\Delta\mathbf{c} & -\Delta\mathbf{d}_2\boldsymbol{\gamma} & -\Delta\mathbf{d}_2\mathbf{K_I} \end{bmatrix};$$

$$\mathbb{B}_1 = \begin{bmatrix} \mathbf{b}_1 - \mathbf{b}_2\boldsymbol{\delta}\Delta\mathbf{d}_1 \\ -\boldsymbol{\beta}\Delta\mathbf{d}_1 \\ -\Delta\mathbf{d}_1 \end{bmatrix}; \quad \mathbb{B}_2 = \begin{bmatrix} \mathbf{b}_2\Delta\boldsymbol{\delta} \\ \boldsymbol{\beta} - \boldsymbol{\beta}\Delta\mathbf{d}_2\boldsymbol{\delta} \\ \mathbf{I}_r - \Delta\mathbf{d}_2\boldsymbol{\delta} \end{bmatrix} \tag{41}$$

$$\mathbb{C}_1 = \begin{bmatrix} \Delta\mathbf{c} & \Delta\mathbf{d}_2\boldsymbol{\gamma} & \Delta\mathbf{d}_2\mathbf{K_I} \end{bmatrix}; \quad \mathbb{D}_{11} = [\Delta\mathbf{d}_1]; \quad \mathbb{D}_{12} = [\Delta\mathbf{d}_2\boldsymbol{\delta}] \tag{42}$$

$$\mathbb{C}_2 = \begin{bmatrix} -\boldsymbol{\delta}\Delta\mathbf{c} & \nabla\boldsymbol{\gamma} & \nabla\mathbf{K_I} \end{bmatrix}; \quad \mathbb{D}_{21} = [-\boldsymbol{\delta}\Delta\mathbf{d}_1]; \quad \mathbb{D}_{22} = [\nabla\boldsymbol{\delta}] \tag{43}$$

$$\Delta = [\mathbf{I}_r - \mathbf{d}_2\boldsymbol{\delta}]^{-1} \quad \nabla = \mathbf{I}_c - \boldsymbol{\delta}\Delta\mathbf{d}_2 \tag{44}$$

The integrals of squared output errors ($I_y$) and squared control signals ($I_u$) allow to quantify the ability of the controller to accurately follow a reference or reject a disturbance and its associated energy usage:

$$I_y = \int_0^\infty (\mathbf{r} - \mathbf{y})^T \mathbb{Q}(\mathbf{r} - \mathbf{y})dt \tag{45}$$

$$I_u = \int_0^\infty (\mathbf{u}_\infty - \mathbf{u})^T \mathbb{R}(\mathbf{u}_\infty - \mathbf{u})dt \tag{46}$$

Here, matrices $\mathbb{Q}$ and $\mathbb{R}$ allow the selection of the desired output or control signal, respectively. García-Alvarado and Ruiz-López (2010) and Vargas-González *et al*. (2013) demonstrated that, if the system does not have steady-state error, indices $I_y$ and $I_u$ are finite and have analytical solutions when step or impulse forcing functions are applied to **r** (servo problem, $\mathbf{r} = \mathbf{k}_2$) and **w** (regulator problem, $\mathbf{r} = \mathbf{k}_1$), eliminating the requirement of performing system simulations. These solutions are given by

$$I_{j-i}^k = \boldsymbol{\Omega}_i^T \mathbb{P}\boldsymbol{\Omega}_i \tag{47}$$

where $i$ represents $r$ (regulator problem) or $s$ (servo problem), $j$ represents $u$ (for control signal) or $y$ (for output error signal) and $k$ represents $p$ (for impulse forcing function) or $s$ (for step forcing function). Matrix $\mathbb{P}$ is evaluated from the following Ricatti equation:

$$\mathbb{A}^T\mathbb{P} + \mathbb{P}\mathbb{A} + \mathbb{V}_k^T\mathbb{C}_j^T\mathbb{X}_j\mathbb{C}_j\mathbb{V}_k = \mathbf{0} \tag{48}$$

where $\boldsymbol{\Omega}_r = \mathbb{B}_1\mathbf{k}_1$, $\boldsymbol{\Omega}_s = \mathbb{B}_2\mathbf{k}_2$, $\mathbb{C}_u = \mathbb{C}_2$, $\mathbb{C}_y = \mathbb{C}_1$, $\mathbb{V}_p = \mathbf{I}$, $\mathbb{V}_s = \mathbf{A}^{-1}$, $\mathbb{X}_u = \mathbb{R}$ and $\mathbb{X}_y = \mathbb{Q}$. Notice that $\mathbf{u}_\infty = 0$ for regulator problems.

Table 1. Controller gains for the Ogunnaike distillation column.

| Parameter | Control settings | | | | | |
|---|---|---|---|---|---|---|
| | WI[1] | VU[2] | KO[3] | XI[4] | DH[5] | LQR[6] |
| $k_{P,11}$ | 0.980 | 2.250 | 0.318 | 1.226 | 1.521 | 0.967 |
| $k_{P,12}$ | -0.698 | 0 | 0 | -0.076 | -0.291 | 0.337 |
| $k_{P,13}$ | 2.10E-2 | 0 | 0 | 1.0E-3 | 5.0E-3 | 8.0E-3 |
| $k_{P,21}$ | 0.351 | 0 | 0 | 0.575 | 0.591 | -4.0E-3 |
| $k_{P,22}$ | -0.638 | -0.49 | -0.191 | -0.221 | -0.386 | -0.444 |
| $k_{P,23}$ | -2.0E-2 | 0 | 0 | 4.70E-4 | -1.0E-3 | -6.0E-3 |
| $k_{P,31}$ | 0.637 | 0 | 0 | 61.10 | 29.22 | -3.764 |
| $k_{P,32}$ | -8.20E-2 | 0 | 0 | 13.94 | 8.928 | -8.831 |
| $k_{P,33}$ | 4.921 | 4.830 | 2.549 | 2.854 | 0.841 | 8.156 |
| $k_{I,11}$ | 0.350 | 0.316 | 5.70E-2 | 0.183 | 0.380 | 0.153 |
| $k_{I,12}$ | -0.388 | 0 | 0 | -2.30E-2 | -7.20E-2 | 3.80E-2 |
| $k_{I,13}$ | -9.0E-3 | 0 | 0 | 2.08E-4 | 1.0E-3 | -2.03E-4 |
| $k_{I,21}$ | 0.209 | 0 | 0 | 0.066 | 0.147 | 2.10E-2 |
| $k_{I,22}$ | -0.478 | -7.60E-2 | -4.70E-2 | -4.40E-2 | -9.60E-2 | -1.086 |
| $k_{I,23}$ | -1.20E-2 | 0 | 0 | 4.31E-5 | -3.0E-4 | -1.0E-3 |
| $k_{I,31}$ | 2.549 | 0 | 0 | 6.744 | 7.306 | 0.144 |
| $k_{I,32}$ | -3.582 | 0 | 0 | 1.966 | 2.232 | -0.386 |
| $k_{I,33}$ | -1.20E-2 | 1.553 | 0.796 | 0.229 | 0.210 | 3.545 |
| $k_{D,11}$ | 1.566 | 5.805 | 6.30E-2 | 0 | 0 | 0.177 |
| $k_{D,12}$ | -0.821 | 0 | 0 | 0 | 0 | 8.0E-2 |
| $k_{D,13}$ | -2.0E-2 | 0 | 0 | 0 | 0 | 5.0E-3 |
| $k_{D,21}$ | -1.571 | 0 | 0 | 0 | 0 | 0.322 |
| $k_{D,22}$ | -1.316 | -1.651 | -0.159 | 0 | 0 | -0.979 |
| $k_{D,23}$ | 3.0E-3 | 0 | 0 | 0 | 0 | -1.40E-2 |
| $k_{D,31}$ | -0.710 | 0 | 0 | 0 | 0 | -0.703 |
| $k_{D,32}$ | -0.889 | 0 | 0 | 0 | 0 | -1.365 |
| $k_{D,33}$ | 4.160 | 49.07 | 0.159 | 0 | 0 | 3.990 |
| $\tau_{11}$ | - | 2.58 | - | - | - | - |
| $\tau_{12}$ | - | 0 | - | - | - | - |
| $\tau_{13}$ | - | 0 | - | - | - | - |
| $\tau_{21}$ | - | 0 | - | - | - | - |
| $\tau_{22}$ | - | 3.37 | - | - | - | - |
| $\tau_{23}$ | - | 0 | - | - | - | - |
| $\tau_{31}$ | - | 0 | - | - | - | - |
| $\tau_{32}$ | - | 0 | - | - | - | - |
| $\tau_{33}$ | - | 10.16 | - | - | - | - |

[1]Iruthayarajan and Baskar (2010). [2]Vu and Lee (2010). [3]Kosáková and Veselý (2007). [4]Xiong *et al*. (2007). [5]Ram and Chidambaram (2015). [6]This work.

On the other hand, if system has steady-state error (as it happens with a proportional controller), the indices $I_y$ and $I_u$ do not reach a limit as $t \to \infty$ and thus an upper limit for integration must be provided. Corresponding solutions in this case are more elaborated and were provided by Estévez-Sánchez *et al*. (2017). The quadratic performance indices $I_y$ and $I_u$ were evaluated for the set-point tracking of different forcing functions where each element in $\mathbf{k}_2 \in \mathbb{R}^{3\times 1}$ belongs to the set $\{-1, 0, 1\}$. A total of 13 reference changes (among 27 possibilities) were obtained in this way as $\mathbf{k}_2 = \mathbf{0}$ is not considered and forcing functions $\mathbf{k}_2$ and $-\mathbf{k}_2$ have the same indices. A final time of 200 min was considered to evaluate the integrals for the proportional controller. Finally, the insensitivity to model uncertainty of

control systems was quantified by the index (Ruiz-López *et al*., 2006):

$$\phi = \max\left[\text{abs}\left(\frac{\text{imag}(\text{eig}(\mathbb{A}))}{\text{real}(\text{eig}(\mathbb{A}))}\right)\right] \tag{49}$$

Minimization of $\phi$ has been shown to reduce the $H_\infty$-norm of the closed-loop and sensitivity transfer matrices, which are classical robustness measures (Ruiz-López *et al*., 2006). Table 1 summarizes selected LQR controller as well as other PI and PID settings reported in literature.

Synthesis of PID controllers based on LQR approach, the estimation of performance indices ($I_y$, $I_u$ and $\phi$) and simulations were performed with the Matlab R2012a (MathWorks Inc., Natick, MA, USA).

#### 2.4.4 *Testing of the robustness properties of control system*

All parameters in Eq. (33) were subjected to a random upward or downward 20% variation of their original values, resulting Eq. (50). Robustness properties of control systems were tested as their ability to stabilize perturbed model (50) while reducing the degradation in quadratic indices of error and control signals in comparison to those obtained with nominal system (33).

$$\mathbf{G}(s) = \begin{bmatrix} \frac{0.528e^{-3.12s}}{5.36s+1} & \frac{-0.732e^{-4.2s}}{10.368s+1} & \frac{-0.00588e^{-0.8s}}{10.872s+1} \\ \frac{0.888e^{-7.8s}}{3.9s+1} & \frac{-2.832e^{-2.4s}}{4.0s+1} & \frac{-0.0144e^{-0.96s}}{5.672s+1} \\ \frac{-27.744e^{-11.04s}}{6.52s+1} & \frac{55.44e^{-11.28s}}{8.72s+1} & \frac{1.044(9.288s+1)e^{-0.8s}}{(3.112s+1)(22.56s+1)} \end{bmatrix} \tag{50}$$

### 2.5 *Adding of derivative action to existing PI controllers for a nonlinear CSTR*

A remarkable characteristic of the proposed methodology is that it can be used to add the derivative action to PI controllers, as described follows. Let us consider a model of a well-mixed nonlinear CSTR with a first order exothermic irreversible reaction and multiple steady-states according with the equations

$$\frac{dC}{dt} = \frac{F}{V}\left(C_f - C\right) - k_0 \exp\left(-\frac{E}{RT}\right)C \tag{51}$$

$$\frac{dT}{dt} = \frac{F}{V}\left(T_f - T\right) + \frac{-\Delta H}{\rho C_P}k_0 \exp\left(-\frac{E}{RT}\right)C \tag{52}$$

being $V$ = 100 L, $C_f$ = 1 mol/L, $k_0$ = 7.2×10$^{-10}$ L/min, $E/R$ = $10^4$ K, $T_f$ = 350 K, $T_{cf}$ = 350 K, $\rho = \rho_c$ = 1000 g/L, $C_p = C_{pc}$ = 1 cal/g/K, $\Delta H$ = −2.5 cal/mol and $h$ = 7×10$^5$ cal/min/K. The feed streams are constrained by $60 \leq F \leq 140$ and $63.41 \leq F_c \leq 103.41$ L/min. Eqs. (51)-(52) have the following state-space representation

$$\begin{bmatrix} x_1 \\ x_2 \end{bmatrix} = \begin{bmatrix} -9.998 & -4.679\times10^{-2} \\ 1799.6 & 7.325 \end{bmatrix}\begin{bmatrix} x_1 \\ x_2 \end{bmatrix} + \begin{bmatrix} 1 & 0 \\ 0 & 1 \end{bmatrix}\begin{bmatrix} w_1 \\ w_2 \end{bmatrix} + \begin{bmatrix} 9\times10^{-3} & 0 \\ -8.854\times10^{-1} & -8.775\times10^{-1} \end{bmatrix}\begin{bmatrix} u_1 \\ u_2 \end{bmatrix} \tag{53}$$

$$\begin{bmatrix} y_1 \\ y_2 \end{bmatrix} = \begin{bmatrix} 1 & 0 \\ 0 & 1 \end{bmatrix}\begin{bmatrix} x_1 \\ x_2 \end{bmatrix} \tag{54}$$

where $x_1 = C - C_{ss}$, $x_2 = T - T_{ss}$, $w_1 = C_f - C_{fss}$, $w_2 = T_f - T_{fss}$, $u_1 = Q - Q_{ss}$, $u_2 = Q_c - Q_{css}$, $y_1 = x_1$ and $y_2 = x_2$. Chen *et al*. (2002) applied a linear matrix inequality (LMI) approach based on $H_\infty$ theory to design a centralized robust PI controller for this CSTR. Later, Ruiz-López *et al*. (2006) found the gains for a robust centralized PI controller by using a multiobjective optimization approach. These controllers are summarized in Table 2 and labeled as CHPI and RLPI, respectively. Centralized derivative action was further added to these controllers using the proposed methodology; the obtained controllers are designated as CHPID and RLPID. In this work, the synthesis of multiloop PID controllers was also explored by using two different approaches. Estévez-Sánchez *et al*. (2017) obtained diagonal versions of the controllers proposed by Chen *et al*. (2002) and Ruiz-López *et al*. (2006), labeled as ESPI1 and ESPI2, respectively. The first approach involves adding the centralized derivative action to the multiloop controllers reported by Estévez-Sánchez *et al*. (2017); thus, diagonalization is applied after the addition of a new action. These controllers are designated as ESPID1 and ESPID2. In the second approach, diagonalization is applied after the full centralized PID controllers are obtained. Here, diagonalization was applied to CHPID and RLPID controllers, resulting in the gain sets DIAG1 and DIAG2, respectively.

Centralized PI controllers consider all input-output interactions. Thus, they are designed without a preconceived proper pairing. However, two-pairings options for the output and control variables exist for the multiloop controllers. Here, only the pairs $\{C, F\}$ and $\{T, F_c\}$ are considered for the diagonalization procedure (the dominant pairing as determined by the RGA method).

Table 2. Controller gains for the CSTR.

| Control settings | $\mathbf{K}_P$ | $\mathbf{K}_I$ | $\mathbf{K}_D$ |
|---|---|---|---|
| CHPI[1] | $\begin{matrix}5783 & 27.81\\ -8724 & -137.7\end{matrix}$ | $\begin{matrix}63687 & 252.6\\ -30645 & -1129\end{matrix}$ | – |
| ESPI1[2] | $\begin{matrix}14778 & 0\\ 0 & -89.20\end{matrix}$ | $\begin{matrix}61083 & 0\\ 0 & -1062\end{matrix}$ | – |
| RLPI[3] | $\begin{matrix}7732 & 0\\ -13770 & -673.6\end{matrix}$ | $\begin{matrix}93938 & 142.3\\ -97506 & -6634\end{matrix}$ | – |
| ESPI2[2] | $\begin{matrix}9967 & 0\\ 0 & -669.5\end{matrix}$ | $\begin{matrix}93092 & 0\\ 0 & -6546\end{matrix}$ | – |
| CHPID[4] | Same as CHPI | | $\begin{matrix}-0.411 & 2.6E-2\\ 617.1 & -0.595\end{matrix}$ |
| ESPID1[4] | Same as ESPI1 | | $\begin{matrix}-3.1E-2 & 0\\ 0 & 3.97E-4\end{matrix}$ |
| RLPID[4] | Same as RLPI | | $\begin{matrix}-12.18 & 2.2E-2\\ 8384 & -10.41\end{matrix}$ |
| ESPID2[4] | Same as ESPI2 | | $\begin{matrix}-9.0E-3 & 0\\ 0 & -147.9\end{matrix}$ |
| DIAG1[5] | $\begin{matrix}1.290 & 0\\ 0 & -91.33\end{matrix}$ | $\begin{matrix}61138 & 0\\ 0 & -1059\end{matrix}$ | $\begin{matrix}1.638 & 0\\ 0 & -5.041\end{matrix}$ |
| DIAG2[6] | $\begin{matrix}9081 & 0\\ 0 & -667.5\end{matrix}$ | $\begin{matrix}93113 & 0\\ 0 & -6544\end{matrix}$ | $\begin{matrix}-0.355 & 0\\ 0 & -13.49\end{matrix}$ |

[1]Chen *et al*. (2002). [2]Estévez-Sánchez *et al*. (2017). [3]Ruiz-López *et al*. (2006). [4]Derivative action added to indicated PI controller. [5]CHPID control after diagonalization procedure. [6]RLPID control after diagonalization procedure.

This pairing was also used by Chen *et al*. (2002) and Estévez-Sánchez *et al*. (2017) to obtain multiloop controllers. Allowable output concentration and temperature errors are around 0.1 mol/L and 5 °C. Then, $q_{11}/q_{22} \approx 100 - 1000$. The quadratic indices $I_y$ and $I_u$ were evaluated for the servo and regulator problems with step forcing functions by using $\mathbf{k}_1^T = \begin{bmatrix} 0.05 & 5 \end{bmatrix}$ and $\mathbf{k}_2^T = \begin{bmatrix} 0.005 & 5 \end{bmatrix}$.

## 2.6 *Convergence of the proposed algorithm*

The estimation of $\mathbf{K}_D$ is based on a fixed-point iteration method, particularly an implicit multivariable implementation. On a general level, the convergence of these methods depends on the form of the iterative function, the derivative of the function at the fixed point and the initial value (Burden and Faires, 2010); however, both the implicit and multivariable form of the iterative matrix function makes extremely difficult, if not impossible, to provide an analytical result of the convergence conditions. In current study, the form of the iterative function is fixed; thus, algorithm convergence can be only controlled trough the initial value. Three different scenarios were explored to force the proposed algorithm to not converge or to produce derivative gains making Ogunnaike system unstable when added to the starting PI gains (a stabilizing controller).

1. Synthesis of derivative action starts from an unstable PID controller (the PI portion stabilize the system but the addition of starting $\mathbf{K}_D$ makes it unstable). Derivative gains were initialized as a destabilizing $\mathbf{K}_D$ set where each gain is a random number between -100 and 100. The same starting $\mathbf{K}_D$ was used with multiple combinations of $\mathbf{R}$. A total of 10 $\mathbf{K}_D$ sets were tested in this way.

2. The algorithm starts from a stabilizing PID controller, where $\mathbf{K}_D$ was generated and tested in the same way as above.

3. $\mathbf{K}_D$ gains are initialized as random numbers between -100 and 100 (the resulting starting control can either stabilize or destabilize the

system). A different starting $\mathbf{K}_D$ was paired with a unique $\mathbf{R}$ in the explored region.

The combinations of $\mathbf{R}$ where the same as the originally explored by setting $\mathbf{K}_D = \mathbf{0}$ (1331 combinations) in Section 2.4.2. A total of 27591 controllers were synthesized in the three scenarios.

## 3 Results and discussion

### 3.1 *Synthesis of centralized PID controller for Oggunaike distillation column*

Quadratic indices $I_y$ and $I_u$ obtained after the synthesis of proportional action were in the ranges of 8685-1.23E5 and 2.90E4-3.04E6, respectively. The proportional controller selected at this stage was obtained under weight elements $\{\log_{10} r_{11}, \log_{10} r_{22}, \log_{10} r_{33}\} = \{1.1, 1.9, -2\}$ with corresponding indices $\{I_y, I_u, \phi\} = \{1.80E4, 8.56E5, 2.693\}$. This controller was further extended with the integral action, resulting in a reduction of the output error ($243.1 \leq I_y \leq 299.9$) and control signal ($2.76E5 \leq I_u \leq 4.12E5$) quadratic indices. The PI controller obtained at this stage has weight elements $\{\log_{10} r_{11}, \log_{10} r_{22}, \log_{10} r_{33}\} = \{3.6, 4.1, -0.1\}$ with corresponding indices $\{I_y, I_u, \phi\} = \{297.6, 3.22E5, 3.819\}$. Finally, the quadratic indices $I_y$ and $I_u$ were in the ranges of 258.3-280.4 and 2.78E5-4.90E5 after synthesis of the derivative action. The derivative gains were obtained using the weight elements $\{\log_{10} r_{11}, \log_{10} r_{22}, \log_{10} r_{33}\} = \{1.1, 0.9, -1.7\}$ with corresponding indices $\{I_y, I_u, \phi\} = \{271.36, 3.26E5, 2.037\}$.

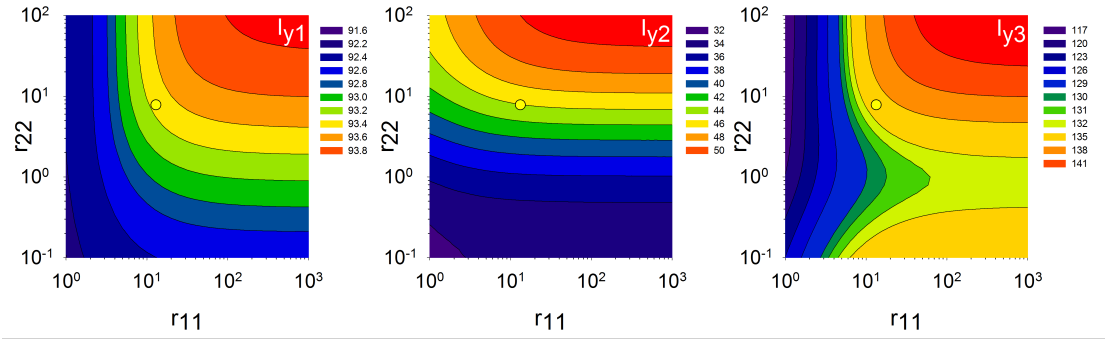


Fig. 1. Effect of the screening of control weights on the resulting quadratic index of each output error during the synthesis of derivative action via LQR approach for the Ogunnaike distillation column. Yellow dot corresponds to selected PID controller with weight elements $\{\log_{10} r_{11}, \log_{10} r_{22}, \log_{10} r_{33}\} = \{1.1, 0.9, -1.7\}$.

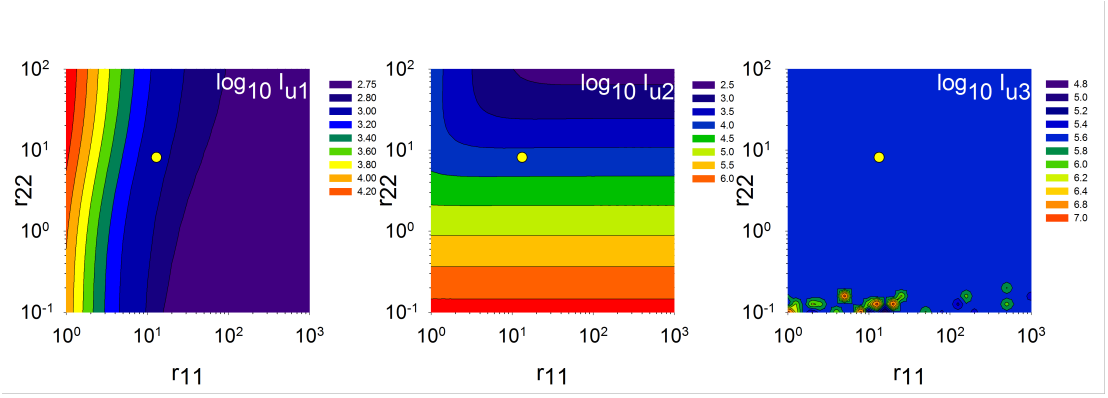


Fig. 2. Effect of the screening of control weights on the resulting quadratic index of each control signal during the synthesis of derivative action via LQR approach for the Ogunnaike distillation column. Yellow dot corresponds to selected PID controller with weight elements $\{\log_{10} r_{11}, \log_{10} r_{22}, \log_{10} r_{33}\} = \{1.1, 0.9, -1.7\}$.

The effect of the screening of control weights on the resulting indices $I_y$ and $I_u$ during the synthesis of the derivative action is shown in figs. 1 and 2, respectively. For clarity purpose, each contribution to the indices is shown. These figures reveal two main characteristics of the quadratic indices: (1) they minimize in different directions and (2) they span different value ranges. The performance of LQR controllers depends on the selection of the control weight matrices determining the trade-off between acceptable output error and magnitude of the control signal. Thus, the synthesis procedure represents a complex multiobjective optimization problem requiring special methodologies to refine further the control characteristics as has been shown in some previous studies (Das *et al*., 2015). Nonetheless, the proposed sequential approach to PID controller synthesis reduces the problem dimension when compared to other methods where optimization occurs in the original space of controller gains. The resulting PID controller gains (labeled as LQR) are summarized in Table 1.

Quadratic indices ($I_y$ and $I_u$) obtained with LQR controller as well as using PI and PID settings reported in literature are shown in Table 2 for nominal (left) and perturbed (right) models. The indices $I_y = 271.36$ and $I_u = 3.26E5$ obtained with the state-space model and analytical solutions are shown as $\{I_{y1}, I_{y2}, I_{y3}\} = \{94.25, 43.98, 133.2\}$ and $\{I_{u1}, I_{u2}, I_{u3}\} = \{718.3, 4767, 3.20E5\}$ for each output and control variable, respectively. These indices are calculated as $\{I_{y1}, I_{y2}, I_{y3}\} = \{96.03, 62.55, 1070\}$ and $\{I_{u1}, I_{u2}, I_{u3}\} = \{572.5, 676.7, 5.52E5\}$ when using original matrix transfer model and numerical integration of simulation results. Differences between indices calculated with analytical and numerical solutions result because process delays are approximated in state-space representation. For the first output, the WI control exhibits the best performance (lowest value) and proposed LQR control is ranked in fifth place. However, the proposed controller is the best ranked for the second and third outputs, while exhibiting a moderate use of the control signals. Table 2 also shows the $\phi$ index, which provides a measure of the robustness properties of the control system, regardless it is calculated for the approximated state-space representation. The lower the $\phi$ value the more insensitive the control system is to model uncertainty (Ruiz-López *et al*., 2006). Thus, this index was also minimized during the synthesis of PID controller via the LQR method to guarantee the selected gains would stabilize not only the state-space model, but also the original transfer matrix model as well as its perturbed version. As expected, the selected LQR controller also stabilized the perturbed model, with a $\phi$ value (2.0) comparable to those of the other stabilizing controllers (1.2-3.4); however, the WI controller, with the highest $\phi$ value (5.1) among all tested settings, failed to stabilize the perturbed model. As a result, these settings were the least robust, even if WI controller achieved a fast reference tracking (low $I_y$ values) for the nominal system. The performance of XI and DH controls (both centralized PI settings) degraded in terms of $I_y$ and $I_u$ for all variables (indices become bigger). VU controller degraded five out of six indices in perturbed model, while remaining controllers (KO and LQR) only degraded four indices. Overall, the controllers ranked in the order KO(0.37%) < VU (6.93%) < DH (35.3%) < LQR (44.5%) < XI (107.3%) in terms of relative degradation of cummulative quadratic index of error ($I_{y1} + I_{y2} + I_{y3}$).

Table 3. Quadratic indices of control systems for the Ogunnaike distillation column.[1]

| Control settings | $I_{y1}$ | $I_{y2}$ | $I_{y3} \times 10^{-3}$ | $I_{u1}$ | $I_{u2}$ | $I_{u3} \times 10^{-5}$ | $\phi$ |
|---|---|---|---|---|---|---|---|
| WI | 57.41/-[2] | 84.22/-[2] | 4.679/-[2] | 1.77E4/-[2] | 2.70E4/-[2] | 101.2/-[2] | 5.105 |
| VU | 50.78/57.61 | 180.8/96.87 | 6.867/7.436 | 187.0/1364 | 127.6/390.9 | 4.085/7.020 | 3.378 |
| KO | 225.0/271.1 | 103.5/68.48 | 1.560/1.556 | 1924/2118 | 529.8/957.0 | 7.232/12.79 | 1.237 |
| XI | 83.05/107.3 | 116.2/189.6 | 29.451/61.16 | 246.5/1357 | 67.98/325.3 | 1.412/3.734 | 1.239 |
| DH | 55.57/71.52 | 103.8/192.1 | 52.180/70.57 | 44.60/1365 | 18.83/251.8 | 1.415/3.396 | 1.197 |
| LQR | 96.03/103.5 | 62.55/38.23 | 1.070/1.633 | 572.5/1470 | 676.7/500.36 | 5.527/8.262 | 2.037 |

[1]Quadratic indices were evaluated with nominal (left values) and perturbed (right values) models. Values represent the sum of indices obtained under the reference changes $\mathbf{k}_2^T$ = [1 0 0], [0 1 0], [0 0 1], [1 1 0], [1 0 1], [0 1 1], [1 -1 0], [-1 0 1], [0 1 -1], [1 1 -1], [1 -1 1], [-1 1 1] and [1 1 1]. Robustness index was evaluated with state-space model. Lower numbers represent better performance.

[2]Unstable process.

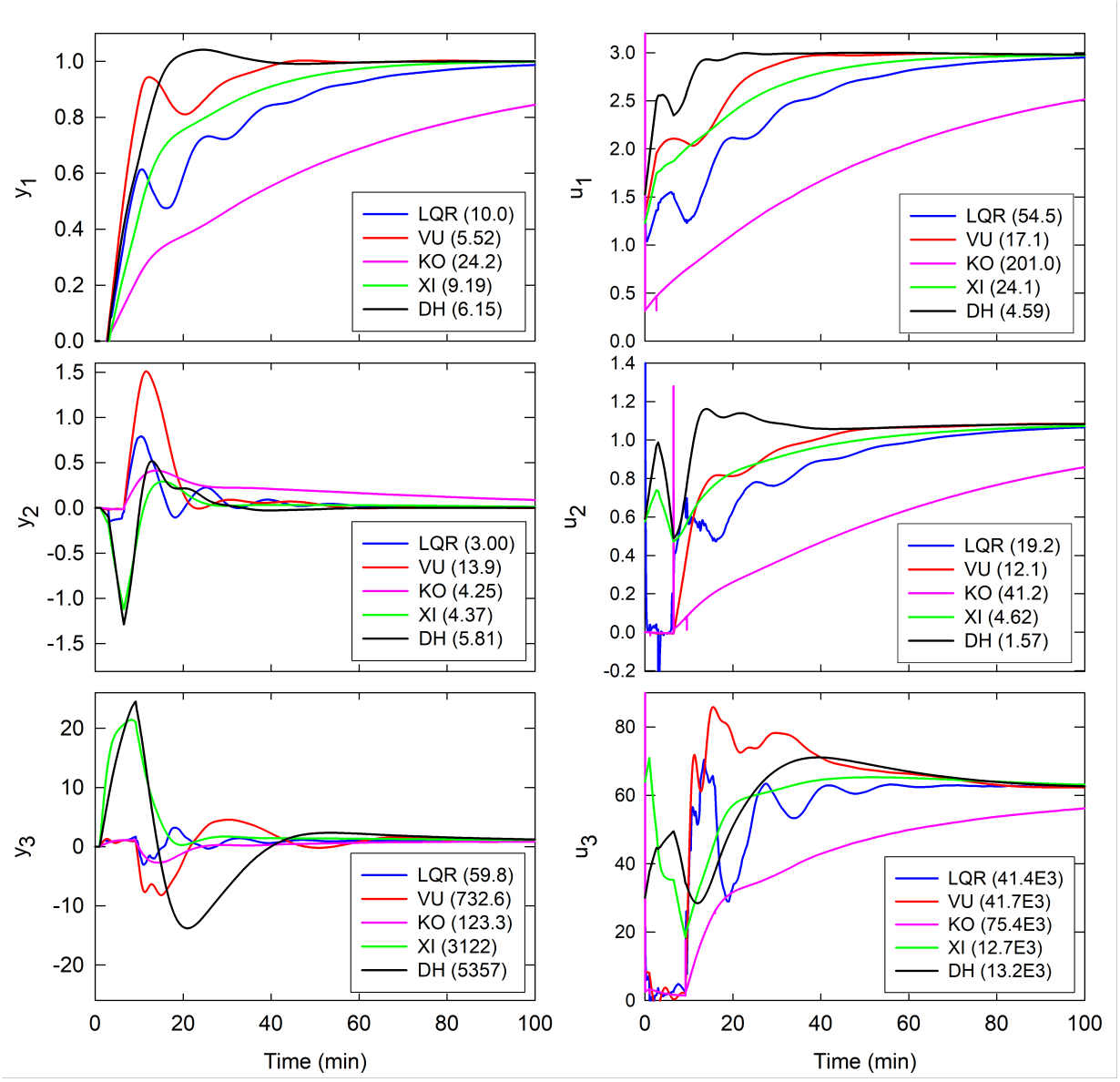


Fig. 3. Response of the Ogunnaike distillation column to a unit-step set-point change in first output ($\mathbf{k}_2^T$ = [1 0 0]). Numbers in parentheses represent the quadratic indices of the plotted variable (lower numbers represent better performance).

On the other hand, the rank became LQR(49.5%) < VU (72.1%) < KO (76.7%) < DH (141.0%) < DH (165.0%) in terms of relative degradation of cummulative quadratic index of control signal ($I_{u1}$ + $I_{u2}$ + $I_{u3}$). Therefore, proposed LQR controller is equilibrated in terms of fast reference tracking, low usage of the control signals and robustness properties. A comparison of selected controllers (LQR, VU, KO, XI and DH) during simulation of a unit step change in first output ($\mathbf{k}_2^T$ = [1 0 0]) is shown in Fig. 3 for the nominal system. Here, the control systems are ranked in the order LQR (72.8) < KO (151.8) < VU (752.1) < XI (3136) < DH (5369) in terms of the quadratic index of output error. On the other hand, they rank as XI (12.7E3) < DH (13.2E3) < LQR (41.4E3) < VU (41.8E3) < KO (75.4E3) in the quadratic index of control signal.

### *3.2 Addition of derivative action to centralized PI control for a CSTR*

The obtained quadratic indices $I_y$ and $I_u$ under both set-point tracking and disturbance rejection scenarios for the original nonlinear model are summarized in Table 4. In general, PID controllers showed better performance indices that their PI counterparts. For example, 20 out of 32 indices improved when centralized or multiloop controllers added with the derivative action (CHPID, RLPID, ESPID1 and ESPID2) were tested in the nonlinear CSTR. Table also shows the quadratic indices for DIAG1 and DIAG2 controllers obtained by diagonalization of their centralized counterparts (CHPID and RLPID), where it is verified that multiloop controllers behave in a similar way as the original ones. The results demonstrate that diagonal PID controllers can be obtained by starting from centralized or diagonal PI gains. An indicative simulation with both setpoint changes ($C = C_{ss} + 0.005$ mol/L and $T = T_{ss} + 5$ K at $t = 0$ min) and input disturbances ($C_f = C_{fss} + 0.05$ mol/L and $T_f = T_{fss} + 5$ K at $t = 1$ min) is presented in Fig. **??** for CHPI, CHPID, RLPI and RLPID controllers. These simulations show that addition of derivative action improved original PI controllers by allowing a tighter set-point tracking while reducing the control signal usage, especially in $F_c$, where it eliminates signal saturation in periods no longer than 30 s. Two main conclusions can be drawn from results presented in this section: (1) the proposed LQR method generalizes other PI controller tuning methodologies by allowing the synthesis of the derivative action and (2) diagonalization procedure allows the development of multiloop controllers behaving in a similar way to their corresponding centralized versions.

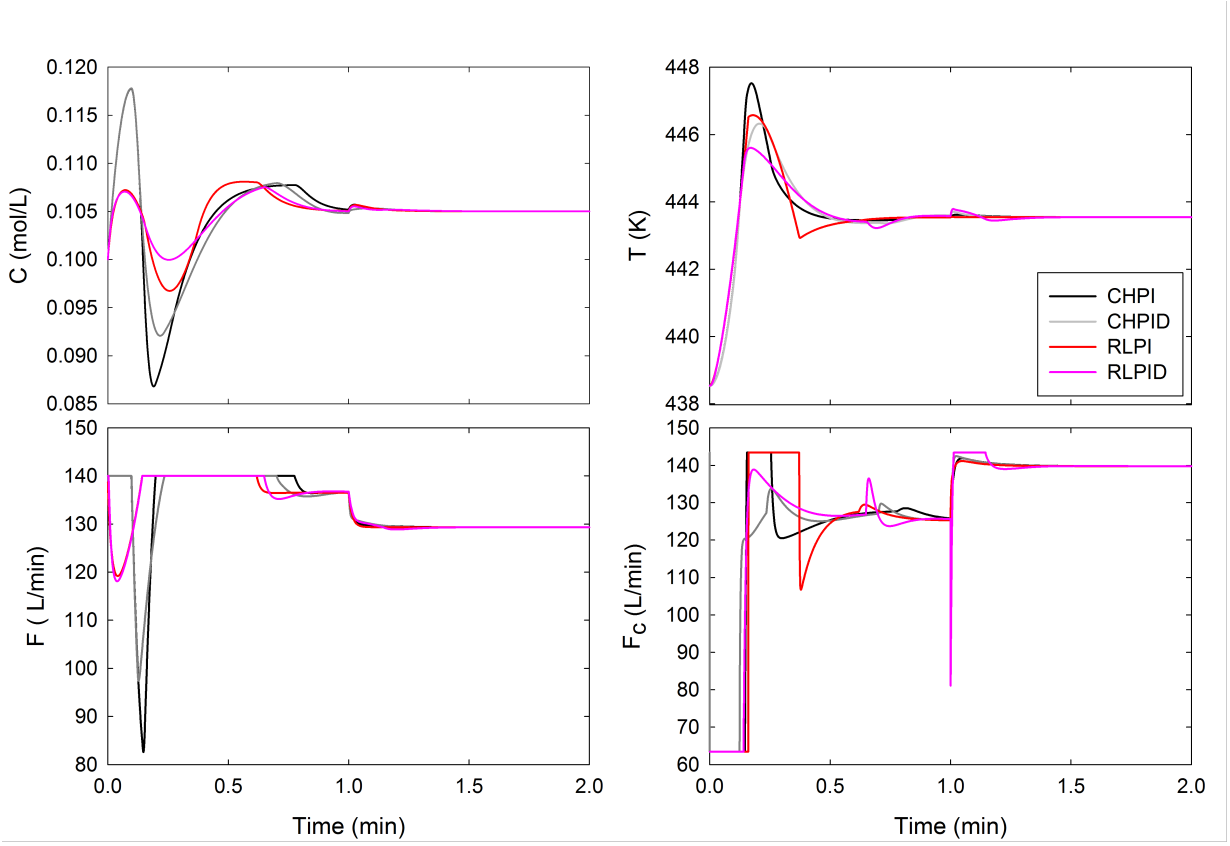


Fig. 4. Response of the nonlinear CSTR to both set-point changes and input disturbances using centralized PI and PID controllers.

Table 4. Quadratic indices of control systems for the CSTR.[1]

| Index | Control settings | | | | | | | | | |
|---|---|---|---|---|---|---|---|---|---|---|
| | CHPI | CHPID | ESPI1 | ESPID1 | DIAG1 | RLPI | RLPID | ESPI2 | ESPID2 | DIAG2 |
| $I^s_{y1-s} \times 10^5$ | 4.597 | 3.481 | 1.506 | 0.8612 | 1.602 | 1.139 | 0.5355 | 0.8417 | 0.6790 | 1.874 |
| $I^s_{y2-s}$ | 2.975 | 2.6943 | 2.605 | 2.011 | 2.683 | 2.449 | 1.937 | 1.976 | 1.821 | 2.972 |
| $I^s_{y1-r} \times 10^8$ | 1.337 | 1.239 | 1.356 | 1.539 | 1.361 | 1.639 | 1.516 | 1.331 | 1.461 | 1.352 |
| $I^s_{y2-r} \times 10^6$ | 223.2 | 295.5 | 664.2 | 663.6 | 674.4 | 2.296 | 713.9 | 13.68 | 0.1432 | 13.91 |
| $I^s_{u1-s}$ | 115.5 | 68.24 | 46.47 | 47.84 | 47.10 | 26.15 | 28.40 | 47.94 | 48.00 | 72.42 |
| $I^s_{u2-s}$ | 602.9 | 485.7 | 725.6 | 561.5 | 735 | 694.3 | 569.9 | 668.6 | 606.4 | 371.0 |
| $I^s_{u1-r} \times 10^1$ | 1.802 | 1.361 | 1.441 | 1.653 | 1.500 | 1.854 | 2.300 | 1.506 | 1.700 | 1.516 |
| $I^s_{u2-r} \times 10^1$ | 6.179 | 21.07 | 11.06 | 3.862 | 19.22 | 2.626 | 76.43 | 3.012 | 2.189 | 1.616 |

[1]Evaluated from the numerical integration of simulation results using original nonlinear system. Lower numbers represent better performance. $u_{1\infty}$ = 136.5 and $u_{2\infty}$ = 125.2 for the servo problem. $u_{1\infty}$ = 94.7 and $u_{2\infty}$ = 114.2 for the regulator problem.

### 3.3 *Effect of starting guess on synthesis of derivative gains*

The derivative action is synthesized on top of a stabilizing PI controller, which can be obtained by solving a non-iterative standard LQR problem (as in the distillation column example) or any other method (as in the CSTR example). The algorithm was initialized by setting $\mathbf{K}_D = \mathbf{0}$ (algorithm starts from a PI control which is let to evolve into a PID one) during screening of control weights for the synthesis of PID controllers (as described in Section 2.4.2) and later tested with random both stabilizing or destabilizing initial $\mathbf{K}_D$ sets (as described in Section 2.6). In all cases, the proposed method neither failed to produce derivative actions causing the system to become unstable or failed to asymptotically approach a limit solution. Moreover, the same stabilizing $\mathbf{K}_D$ was obtained no matter the starting value for a given control weight matrix $\mathbf{R}$.

## 4 Conclusions

The LQR methodology was generalized to allow tuning of centralized PID controllers with better characteristics for set-point tracking, disturbance rejection, limited use of control signal and insentivity to plant model uncertainty than several previosly reported methods. The sequential nature of the proposed approach allows adding the derivative action to existing PI controllers tuned with other methodologies, enhancing their operation and obtaining simplified multiloop structures from centralized controllers while mostly retaining their original characteristics.

### *Acknowledgments*

Miguel Ángel Hernández-Osorio acknowledges his post-graduate scholarship from CONACYT (Grant No. 856211). Dr. Irving Israel Ruiz-López would like to thank the VIEP-BUAP (100474666-VIEP2019) for providing financial support through the *Programa Institucional para la Consolidación de los Cuerpos Académicos y Conformación de Redes de Investigación*.

### *Nomenclature*

| | |
|---|---|
| $\mathbf{a}$,$\hat{\mathbf{a}}$,$\mathbf{b}_1$, $\mathbf{b}_2$,$\hat{\mathbf{b}}_2$,$\mathbf{c}$, $\mathbf{d}_1$,$\mathbf{d}_2$,$\mathbf{f}$ | open-loop state-space matrices |
| $\mathbf{A}$,$\mathbf{B}_1$,$\mathbf{B}_2$, $\mathbf{C}$ | LQR state-space matrices |
| $\mathbb{A}$,$\mathbb{B}_1$,$\mathbb{B}_2$, $\mathbb{C}_1$,$\mathbb{C}_2$, $\mathbb{D}_{11}$, $\mathbb{D}_{12}$,$\mathbb{D}_{21}$, $\mathbb{D}_{22}$ | closed-loop state-space matrices |
| $c$,$C$ | number of control variables |
| $\mathbf{D}$ | eigenvalues of $\mathbf{K}_P$, $\mathbf{K}_I$ or $\mathbf{K}_D$ ($\mathbb{R}^{c\times r}$, $c = r$) |
| $\mathbf{e}$ | error vector ($\mathbb{R}^{o\times 1}$) |
| $I$ | quadratic performance index |
| $J$ | quadratic performance index for LQR problem |
| $\mathbf{K}$ | state feedback gains in LQR problem solution |
| $k$ | a given element in either $\mathbf{K}_P$, $\mathbf{K}_I$ or $\mathbf{K}_D$ |
| $\mathbf{k}_1$ | magnitude for forcing function in regulator problem |
| $\mathbf{k}_2$ | magnitude for forcing function in servo problem |
| $\mathbf{K}_P$, $\mathbf{K}_I$,$\mathbf{K}_D$ | proportional, integral and derivative gain matrices |

| | |
|---|---|
| $n$,$N$ | number of state variables |
| $o$,$O$ | number of measured output variables |
| $m$, $M$ | number of exogenous variables |
| $\mathbf{P}$ | solution to Riccati equation in LQR problem $\mathbb{R}^{N\times N}$ |
| $\mathbf{q}$ | integral output state ($\mathbb{R}^{o\times 1}$) |
| $\mathbf{Q}$, $\hat{\mathbf{Q}}$ | output weight matrices: original ($R^{c\times r}$) and LQR ($\mathbb{R}^{c\times r}$) representations, r espectively |
| $\mathbb{Q}$ | output weight matrix for closed-loop response |
| $\mathbf{r}$ | reference vector ($\mathbb{R}^{r\times 1}$) |
| $\mathbf{R}$, $\hat{\mathbf{R}}$ | control weight matrices: original($\mathbb{R}^{r\times r}$) and LQR ($\mathbb{R}^{r\times r}$) representations, respectively |
| $\mathbb{R}$ | control weight matrix for closed-loop response ($\mathbb{R}^{c\times c}$) |
| $s$,$S$ | number of control state variables |
| $t$ | time |
| $\mathbf{V}$ | eigenvectors of $\mathbf{K}_P$, $\mathbf{K}_I$ or $\mathbf{K}_D$ ($\mathbb{R}^{c\times r}$, $c = r$) |
| $\mathbf{u}$,$\mathbf{U}$ | control vectors: original ($\mathbb{R}^{c\times 1}$) and LQR ($\mathbb{R}^{C\times 1}$) systems, respectively |
| $\mathbf{w}$,$\mathbf{W}$ | exogenous signal vectors: original ($\mathbb{R}^{m\times 1}$) and LQR ($\mathbb{R}^{M\times 1}$) systems, respectively |
| $\mathbf{x}$,$\mathbf{X}$ | open-loop state vectors: original ($\mathbb{R}^{n\times 1}$) and LQR ($\mathbb{R}^{N\times 1}$) systems, respectively |
| $\mathbf{y}$,$\mathbf{Y}$ | measured output vectors: original ($\mathbb{R}^{o\times 1}$) and LQR ($\mathbb{R}^{O\times 1}$) systems, respectively |
| $\mathbf{z}$ | closed-loop state vector ($\mathbb{R}^{(n+s+r)\times 1}$) |

*Greek symbol*

| | |
|---|---|
| $\boldsymbol{\alpha}$,$\boldsymbol{\beta}$,$\boldsymbol{\gamma}$,$\boldsymbol{\delta}$ | control state-space matrices |
| $\phi$ | robustness index |
| $\tau$ | filter time constant |
| $\xi$ | control state ($\mathbb{R}^{s\times 1}$) |

*Subscripts*

| | |
|---|---|
| $\infty$ | final steady-state |
| $I$ | for integral action |
| $P$ | for proportional action |
| $D$ | for derivative action |
| $r$ | for regulator problem |
| $s$ | for servo problem |
| $ss$ | for steady-state |
| $u$ | for control signal |
| $y$ | for output signal |

*Superscripts*

| | |
|---|---|
| $p$ | for an impulse forcing function |
| $s$ | for a step forcing function |

## References


Besta, C.S. (2018). Multi-centralized control system design based on equivalent transfer functions using gain and phase-margin specifications for unstable TITO process. *International Journal of Dynamics and Control 6*, 817-826.

Burden, R.L., Faires, J.D. (2010). *Numerical Analysis. Ninth edition.* Cengage Learning. Canada.

Chen, C.-L., Wang, T.-C., Hsu, S.-H. (2002). An LMI approach to $H_\infty$ PI controller design. *Journal of Chemical Engineering of Japan 35*, 83-93.

Cruz-Rojas, A., Rumbo-Morales, J.Y., de la Cruz-Soto, J., Brizuela-Mendoza, J.A., Sorcia-Vázquez, F.D.J., Martínez-García, M. (2019). Simulation and control of reactants supply and regulation of air temperature in a PEM fuel cells system with capacity of 50 kW. *Revista Mexicana de Ingeniería Química 18*, 349-360.

Das, S., Pan, I., Das, S.(2015). Multi-objective LQR with optimum weight selection to design FOPID controllers for delayed fractional order processes. *ISA Transactions 58*, 35-49.

Das, S., Pan, I., Halder, K., Das. S. Gupta, A. (2013). LQR based improved discrete PID controller design via optimum selection of weighting matrices using fractional order integral performance index. *Applied Mathematical Modelling 37*, 4253-68.

Estévez-Sánchez, K.H., Sampieri-Croda, A., García-Alvarado, M.A., Ruiz-López, I.I. (2017). Design of multiloop PI controllers based on quadratical optimal approach. *ISA Transactions 70*, 338-347.

Flores-Estrella, R.A., Estrada-Baltazar, A., Femat, R. (2016). A mathematical model and dynamic analysis of anaerobic digestion of soluble organic fraction of municipal solid waste towards control design. *Revista Mexicana de Ingeniería Química 15*, 243-258.

García-Alvarado, M.A., Ruiz-López, I.I. (2010). A design method for robust and quadratic optimal MIMO linear controllers. *Chemical Engineering Science 65*, 3431-8.

He, J.-B., Wang, Q.-G., Lee, T.-H. (2000). PI/PID controller tuning via LQR approach. *Chemical Engineering Science 55*, 2429-2439.

Iruthayarajan, M.W., Baskar, S. (2010). Covariance matrix adaptation evolution strategy based design of centralized PID controller. *Expert Systems with Applications 37*, 5775-5781.

Kozáková, A., Veselý, V. (2007). Improved tuning technique for robust decentralized PID controllers. *IFAC Proceedings Volumes 40*, 61-66.

Liu, Y., Gao, Y., Gao, Z., Wang, H., Li, P. (2010). Simple nonlinear predictive control strategy for chemical processes using sparse kernel learning with polynomial form. *Industrial and Engineering Chemistry Research 49*, 8209-8218.

Ma, D., Chen, J., Liu, A., Chen, J., Niculescu, S.-I. (2019). Explicit bounds for guaranteed stabilization by PID control of second-order unstable delay systems. *Automatica 100*, 407-411.

Maghade, D.K., Patre, B.M. (2012). Decentralized PI/PID controllers based on gain and phase margin specifications for TITO processes. *ISA Transactions 51*, 550-558.

Nandong, J., Zang, Z. (2014). Multi-loop design of multi-scale controllers for multivariable processes. *Journal of Process Control 24*, 600-612.

Ogunnaike, B.A., Lemaire, J.P., Morari, M., Ray, W.H. (1983). Advanced multivariable control of pilot-plant distillation column. *AIChE Journal 29*, 632-640.

Pathiran, A.R., Jagadeesan, P. (2018). Model based multivariable control scheme in a reset configuration for stable multivariable systems. *The Canadian Journal of Chemical Engineering 96*, 1317-1326.

Ram, V.D., Chidambaram, M. (2015). Simple method of designing centralized PI controllers for multivariable systems based on SSGM. *ISA Transactions 56*, 252-260.

Rodríguez-Mariano, A., Reynoso-Meza, G., Páramo-Calderón, D.E., Chávez-Conde, E., García-Alvarado, M.A., Carrillo-Ahumada, J. (2015). Comparative performance analysis of different linear controllers tuned for several Cholette's bioreactor steady states using multi-criteria decision making techniques. *Revista Mexicana de Ingeniería Química 14*, 167-204.

Ruiz-López, I.I., Rodríguez-Jimenes, G.C., García-Alvarado, M.A. (2006). Robust MIMO PID controllers tuning based on complex/real ratio of the characteristic matrix eigenvalues. *Chemical Engineering Science 61*, 4332-4340.

Salazar-Pereyra, M., Lugo-Leyte, R., Bonilla-Blancas, A.E., Méndez-Lavielle, F., Lugo-Méndez, H.D. (2016). Theoretical analysis of thermal control of evaporator of refrigeration system with HFC-134a. *Revista Mexicana de Ingeniería Química 15*, 291-297.

Srivastava, S., Misra, A., Thakur, S.K., Pandit, V.S. (2016). An optimal PID controller via LQR for standard second order plus time delay systems. *ISA Transactions 60*, 244-253.

Vargas-Gonzales, S., Rodríguez-Jimenes, G.C., García-Alvarado, M.A., Carrillo-Ahumada, J. (2013). Relation between first order dynamic parameters with PI control parameters in Nash equilibrium. In: Proceedings of the International Conference on Mechatronics, Electronics and Automotive Engineering. *ICMEAE*, 123-6.

Vu, T.N.L., Lee, M. (2010). Independent design of multi-loop PI/PID controllers for interacting multivariable processes. *Journal of Process Control 20*, 922-933.

Xiong Q., Wen-Jian., C., Mao-Jun., H. (2007). Equivalent transfer function method for PI/PID controller design of MIMO processes. *Journal of Process Control 17*, 665-673.